IOPscience iopscience.iop.org

Home Search Collections Journals About Contact us My IOPscience

Magnetic interactions in equi-atomic rare-earth intermetallic alloys RScGe (R = Ce, Pr, Nd and Gd) studied by time differential perturbed angular correlation spectroscopy and *ab initio* calculations

This article has been downloaded from IOPscience. Please scroll down to see the full text article.

2009 J. Phys.: Condens. Matter 21 115601

(http://iopscience.iop.org/0953-8984/21/11/115601)

View the table of contents for this issue, or go to the journal homepage for more

Download details:
IP Address: 129.252.86.83
The article was downloaded on 29/05/2010 at 18:38

Please note that terms and conditions apply.

IOP PUBLISHING JOURNAL OF PHYSICS: CONDENSED MATTER

J. Phys.: Condens. Matter **21** (2009) 115601 (11pp) doi:10.1088/0953-8984/21/11/115601

Magnetic interactions in equi-atomic rare-earth intermetallic alloys RScGe (R = Ce, Pr, Nd and Gd) studied by time differential perturbed angular correlation spectroscopy and *ab initio* calculations

S N Mishra

Department of Nuclear and Atomic Physics, Tata Institute of Fundamental Research, Homi Bhabha Road, Mumbai 400005, India

E-mail: mishra@tifr.res.in

Received 6 November 2008, in final form 31 January 2009
Published 20 February 2009
Online at stacks.iop.org/JPhysCM/21/115601

Abstract

Applying the time differential perturbed angular correlation (TDPAC) technique we have measured electric and magnetic hyperfine fields of the ^{111}Cd impurity in equi-atomic rare-earth intermetallic alloys RScGe (R = Ce, Pr and Gd) showing antiferro- and ferromagnetism with unusually high ordering temperatures. The Cd nuclei occupying the Sc site show high magnetic hyperfine fields with saturation values $B_{hf}(0) = 21$ kG, 45 kG and 189 kG in CeScGe, PrScGe and GdScGe, respectively. By comparing the results with the hyperfine field data of Cd in rare-earth metals and estimations from the RKKY model, we find evidence for the presence of additional spin density at the probe nucleus, possibly due to spin polarization of Sc d band electrons. The principal electric field gradient component V_{zz} in CeScGe, PrScGe and GdScGe has been determined to be 5.3×10^{21} V m^{-2}, 5.5×10^{21} V m^{-2} and 5.6×10^{21} V m^{-2}, respectively. Supplementing the experimental measurements, we have carried out *ab initio* calculations for pure and Cd-doped RScGe compounds with R = Ce, Pr, Nd and Gd using the full potential linearized augmented plane wave (FLAPW) method based on density functional theory (DFT). From the total energies calculated with and without spin polarization we find ferrimagnetic ground states for CeScGe and PrScGe while NdScGe and GdScGe are ferromagnetic. In addition, we find a sizable magnetic moment at the Sc site, increasing from $\approx$0.10 μ_B in CeScGe to $\approx$0.3 μ_B in GdScGe, confirming the spin polarization of Sc d band electrons. The calculated electric field gradient and magnetic hyperfine fields of the Cd impurity closely agree with the experimental values. We believe spin polarization of Sc 3d band electrons, strongly hybridized with spin polarized 5d band electrons of the rare-earth, enables a long range Ruderman–Kittel–Kasuya–Yosida (RKKY) interaction between RE 4f moments which in turn leads to high magnetic ordering temperatures in RScGe compounds.

1. Introduction

The magnetic behavior of rare-earth intermetallic compounds of the type RTX, where R is a rare-earth, T is a transition 3d element and X belongs to the p-group of elements, has been attracting considerable interest during the past several years [1]. The compounds crystallizing in the La_2Sb-type tetragonal structure, show ferro-or antiferromagnetic ordering with unusually high transition temperatures [2–5]. For example, GdScGe has been reported to be a strong ferromagnet [2, 6] with $T_c \approx 350$ K while CeScGe shows antiferromagnetism with $T_N = 46$ K [3, 4]. The compound PrScGe has been shown to exhibit multiple magnetic ordering with transition temperatures ranging from 80–140 K [5].

 © 2009 IOP Publishing Ltd Printed in the UK

Considering that the magnetism in these alloys arises mainly due to the RKKY interaction between the moments on the rare-earth atoms which are separated by a large R–R distance $d > 3.85$ Å, it is surprising that the compounds show such high magnetic ordering temperatures. Recently, from electronic structure calculations using the tight binding linear muffin tin orbital (TB-LMTO) method performed for the structurally similar compounds GdTiGe and GdTiSi Skorek *et al* [7] have suggested that spin polarization of Ti 3d band electrons might be responsible for the high ferromagnetic ordering temperatures of these alloys. In view of the above suggestion spin polarization of Sc 3d band electrons may also play an important role in the occurrence of high magnetic ordering temperatures in RScGe compounds. Thus experimental and theoretical studies dedicated to study Sc spin polarization in RScGe compounds are desirable. Experimentally, hyperfine field measurements using nuclear techniques, namely time differential perturbed angular correlation/distribution (TDPAC/TDPAD) are excellent tools for microscopic investigation of spin correlation in magnetic materials [8–10]. Although TDPAC measurements are possible using a ^{44}Sc probe, the signal-to-noise ratio for this case has been found to be poor. As such, it has scarcely been used for studying magnetic interactions in alloys [11]. Similarly, TDPAD measurements using a recoil-implanted ^{43}Sc probe produced via heavy ion nuclear reaction is difficult in multi-element intermetallic alloys because of the large background arising from unwanted gamma rays. In addition, the severe radiation damage induced by swift heavy ions pose a serious problem in the observation of spin rotation, rendering the method unsuitable for magnetic studies in intermetallic alloys. As an alternative approach, one can measure the transferred hyperfine field for radionuclei like ^{111}Cd using the TDPAC method. This has been found to be extremely useful for detecting spin polarization in different magnetic materials [8–10]. Recently, we have applied the TDPAC technique to study the magnetic interaction in ferromagnetic NdScGe with $T_C \approx 200$ K. The observation of a large hyperfine field B_{hf} at the ^{111}Cd probe indicated that the Sc d band in the alloy might be spin polarized [12]. In this regard, systematic microscopic investigations in other RScGe compounds are highly desirable.

In this paper we present our results on the electric and magnetic hyperfine fields of ^{111}Cd nuclei in antiferromagnetic CeScGe and PrScGe, and ferromagnetic GdScGe. The results obtained from time differential perturbed angular correlation (TDPAC) measurements show large magnetic hyperfine fields with saturation values $B_{hf}(0) = 21$ kG, 45 kG and -189 kG in the Ce, Pr and Gd compounds, respectively. The B_{hf} of ^{111}Cd in RScGe alloys, much higher than the values observed in the corresponding rare-earth (RE) metals, indicate the presence of additional spin density at the probe nucleus, possibly due to spin polarization of Sc d band electrons. Supplementing the experimental studies, we have carried out *ab initio* calculations for pure and Cd-doped RScGe compounds with R = Ce, Pr, Nd and Gd using the full potential linearized augmented plane wave (FLAPW) method based on density functional theory (DFT). From the total energies calculated with and without spin polarization we find ferrimagnetic ground states for CeScGe and PrScGe while NdScGe and GdScGe are ferromagnetic. In addition, we find a sizable magnetic moment at the Sc site, increasing from $\approx 0.10\ \mu_B$ in CeScGe to $\approx 0.3\ \mu_B$ in GdScGe, confirming the spin polarization of Sc d band electrons. The calculated electric field gradient and magnetic hyperfine fields of the Cd impurity closely agree with the experimental values.

2. Experimental details

Polycrystalline alloys of CeScGe, PrScGe and GdScGe were prepared by arc melting the stoichiometric amounts of high purity constituent elements in an argon atmosphere followed by annealing at 1050 °C for 10 days. For GdScGe, a slight off-stoichiometric composition ($Gd_{1.02}Sc_{0.98}Ge$) was taken to avoid the formation of the unwanted $(GdSc)_5Ge_3$ phase [2]. The samples were characterized by room temperature powder x-ray diffraction measurement and were found to be single phase with CeScSi/La_2Sb-type tetragonal structure (space group $I4/mmm$). The lattice parameters were found to be: $a = 4.345(1)$ Å, $c = 15.943(2)$ Å; $a = 4.331(1)$ Å, $c = 15.890(3)$ Å; and $a = 4.258(2)$ Å, $c = 15.595(3)$ Å for CeScGe, PrScGe and GdScGe, respectively, which are consistent with the values reported earlier [2, 4, 5]. The magnetic transition temperatures were confirmed from bulk magnetization measurements using a superconducting quantum interference device (SQUID) magnetometer from Quantum Design.

Microscopic investigation of the magnetic properties of RScGe compounds with R = Ce, Pr and Gd was carried out by measuring the hyperfine field of ^{111}Cd nuclei using the time differential perturbed angular correlation (TDPAC) technique. For the PAC measurements a trace quantity of commercially available radioactive $^{111}InCl_3$ was introduced into a small piece of the samples by thermal diffusion at 900° for 24 h. The typical concentration of Cd in the sample remains $\leqslant 1$ ppm and thus does not alter the bulk properties of the alloy. The PAC measurements were carried out using the 247–174 keV γ–γ cascade in ^{111}Cd nuclei produced via the electron capture (EC) decay of the parent ^{111}In. For the detection of hyperfine interactions we have used the 247 keV, $I^\pi = 5/2^+$ state in ^{111}Cd with a half-life $T_{1/2} = 84$ ns, nuclear quadrupole moment $Q = 0.8$ b and a magnetic moment $\mu_I = -0.7656\ \mu_N$ [13]. The electric and magnetic hyperfine interactions, manifested as time-dependent modulations in the lifetime decay of the intermediate $5/2^+$ state, were extracted by recording the time spectra in a set-up consisting of four BaF_2 detectors and a standard slow fast coincidence circuit having a time resolution better than 700 ps. The detectors were placed in the standard 90°–180° geometry. The perturbation factor $A_{22}G_{22}(t)$ in the angular correlation function $W(\theta, t) = \sum_{kk} A_{kk} G_{kk}(t) P_k(\cos\theta)$ was obtained by constructing the appropriate ratio function, called the PAC time spectrum [8–10]:

$$R(t) = \frac{2[W(180°, t) - W(90°, t)]}{[W(180°, t) + 2W(90°, t)]}, \qquad (1)$$

where $W(\theta, t)$ are the background-subtracted normalized coincidence counts of the detectors placed at 180° and 90°. Measurements were performed at different temperatures in the range 25–450 K using a closed cycle He refrigerator and specially designed furnace for PAC measurements.

Above the magnetic ordering temperatures, the Cd nuclei are subjected to a pure quadrupole interaction in which case the perturbation function $G_{22}(t)$ is expressed as [8, 14–16]

$$G_{22}(t) = \mathrm{e}^{-\lambda t}\left[S_{20}(\eta) + \sum_{n=1}^{3} S_{2n}(\eta)\cos(\omega_n t) g(\omega_n \delta t)\right], \quad (2)$$

where S_{20} is a constant known as the hard core contribution, S_{2n} are the amplitudes of the primary quadrupole interaction frequencies ω_n and $g(\omega_n\delta, t)$ describes the damping due to static distribution in ω_n arising from random inhomogeneities in the local environment of the probe nuclei which, conventionally, is assumed to be either Lorentzian or Gaussian with δ being the distribution width. The exponential damping term in the equation takes account of possible dynamic fluctuations in the interaction. In general, the quadrupole interaction frequencies are expressed as $\omega_n = b_{2n}(\eta)\omega_0$, where ω_0 is the fundamental frequency related to the principal component V_{zz} of the electric field gradient tensor. For half-integer nuclear spins, e.g. ^{111}Cd, ω_0 is related to V_{zz} by the relation [14]

$$\omega_0 = 6\omega_Q = \frac{6eQV_{zz}}{4I(2I-1)\hbar}. \quad (3)$$

Here, η is the asymmetry parameter of the EFG tensor usually expressed as $\eta = \frac{V_{yy}-V_{xx}}{V_{zz}}$ with $V_{zz} > V_{yy} > V_{xx}$ and $0 \leqslant \eta \leqslant 1$. The coefficients b_{2n} are well-known functions of EFG asymmetry with $b_{2n} = n$ for $\eta = 0$ [14].

In the case of static magnetic interaction the perturbation function $G_{22}(t)$ for the $I = 5/2$ case of ^{111}Cd has a rather simple form [14]:

$$G_{22}(t) = [1/5 + (2/5)\cos(\omega_L t) g(\omega_L \delta t) + (2/5)\cos(2\omega_L t) g(2\omega_L \delta t)], \quad (4)$$

where $\omega_L = g_N \mu_N B_{eff}/\hbar$ is the Larmor frequency due to magnetic hyperfine interaction between the nuclear moment μ_N of the intermediate state and the effective magnetic field $B_{eff} = B_{app} + B_{hf}$ acting on the probe nuclei. Here, $g(\omega_L, \delta, t)$ represents the distribution in Larmor frequency having a width of δ. In reality, however, the quadrupole interaction in the magnetically ordered state may not be zero and one has to consider the combined influence of quadrupole and magnetic interactions on the perturbation function. In such a case the perturbation function is more complex but has the general form [17]

$$G_{22}(t) = \left[a_0(\eta, y, \beta) + \sum_n a_n(\eta, y, \beta)\cos(\omega_0 t) g(\omega_0 \delta t)\right], \quad (5)$$

where the number of frequency components ω_n and their amplitudes a_n depend on the relative strength of the magnetic and quadrupole interactions defined by the ratio $y = \omega_B/\omega_Q$ and the angle β between the magnetic field and the EFG axis. The $G_{22}(t)$ for combined interactions are generally solved numerically by varying y and β.

3. Results and discussion

Figure 1 displays some typical PAC spectra for ^{111}Cd in RScGe alloys for R = Ce, Pr and Gd recorded at different temperatures. The spectra recorded in all the samples show nearly full anisotropy, indicating that the probe ^{111}Cd atoms occupy a unique lattice site, most likely substitutional. From a comparison of the chemical behavior and ionic radius of the mother isotope ^{111}In and the atomic species of the sample under investigation, it is easy to exclude a substitutional Ge site, but one cannot readily discriminate between Sc and the rare-earth sites. However, since the ionic radius of In^{3+} is much closer to the value of Sc^{3+} rather than the rare-earth ions, the ^{111}In probe is likely to substitute preferably at the Sc site. Furthermore, *ab initio* calculations of electric field gradient of the Cd impurity substituted at the Sc site, discussed below, show good agreement with the measured values, thus supporting the above lattice site assignment.

The spectra recorded above the magnetic ordering temperatures of the alloys exhibit pure quadrupole interaction which could be simulated with a unique randomly oriented electric field gradient V_{zz}. The room temperature quadrupole interaction frequencies for ^{111}Cd in CeScGe, PrScGe and GdScGe were found to be $\omega_0 = \approx$91.6(10) MHz, 98.5(10) MHz and 107 MHz, respectively. The corresponding V_{zz} values were estimated to be 4.78×10^{21} V m^{-2}, 5.14×10^{21} V m^{-2} and 5.58×10^{21} V m^{-2}, respectively. Figure 2 displays the temperature dependence of the quadrupole interaction frequency for ^{111}Cd in CeScGe, PrScGe and GdScGe. The ω_0 in Ce and Pr compounds increase with decreasing temperature while the same in GdScGe is found to be temperature-independent. For the Cd in CeScGe and PrScGe, the observed temperature variation ($T > T_c$ or T_N) in ω_0 could be fitted to

$$\omega_0(T) = \omega_0(0)(1 - BT^{\alpha}) \quad (6)$$

yielding $\omega_0 = 101.4$ MHz, $B = 1.9 \times 10^{-5}$ and $\alpha = 1.47$ for CeScGe. The corresponding values for PrScGe came out to be $\omega_0 = 106.6$ MHz, $B = 1.4 \times 10^{-5}$ and $\alpha = 1.5$. The measured temperature dependence is consistent with the usual $T^{3/2}$ behavior observed in metallic systems, ascribed to lattice vibrations [18, 19]. In GdScGe, the observed temperature-independent quadrupole interaction is indicative of weak lattice vibration (small mean square displacement $\langle r^2 \rangle$) possibly due to higher Debye temperature θ_D. As another interesting feature, the quadrupole frequency of Cd in PrScGe was found to decrease again below the ferromagnetic ordering temperature 80 K. A similar decrease in ω_0 has also been reported for Cd in NdScGe [12] which was attributed to possible softening of the lattice near the magnetic ordering temperature. However, recent neutron diffraction measurements did not find any change in lattice parameter near T_c [43]. A decrease in quadrupole interaction in these tetragonal rare-earth compounds can also arise from crystal field effects (CEF), which are likely to be strong for Pr and Nd ions but weak for Gd. A strong influence of CEF on the quadrupole interaction has also been reported from TDPAC measurements in RAl_2 and RAl_3 intermetallic alloys [20].

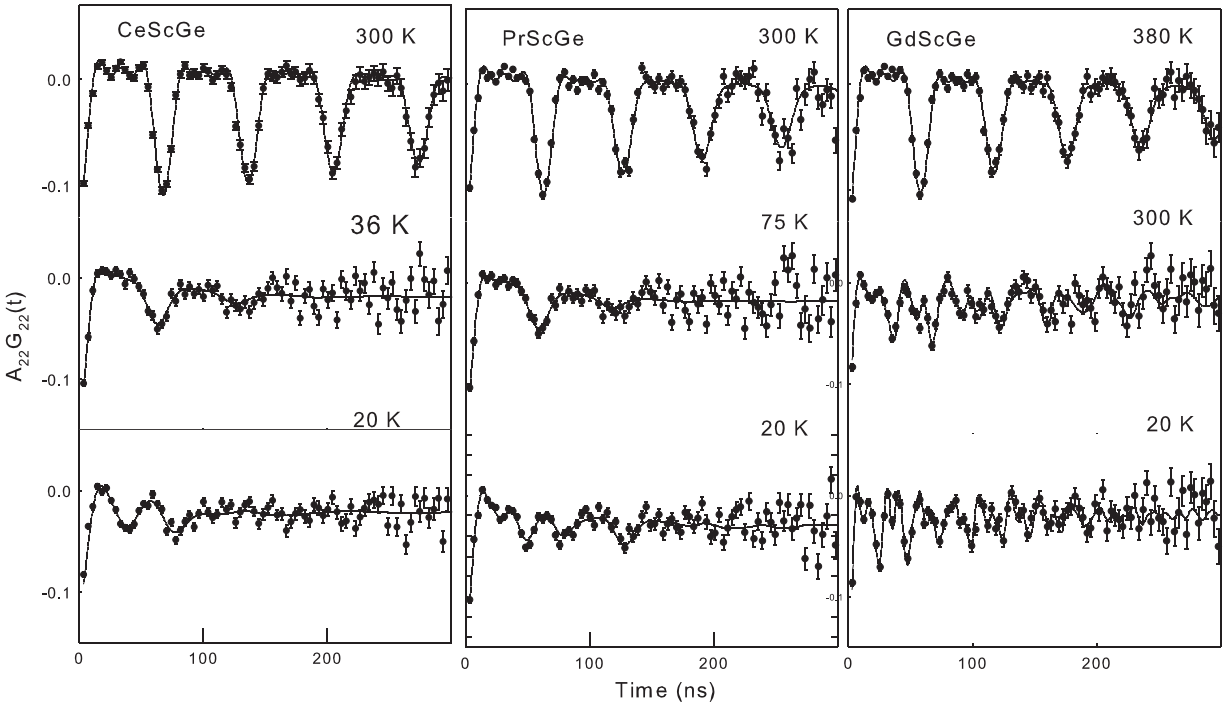

Figure 1. Typical TDPAC spectra for ^{111}Cd in RScGe (R = Ce, Pr and Gd) recorded at different temperatures and zero external field. The solid lines are fits to appropriate G_{22} functions discussed in the text.

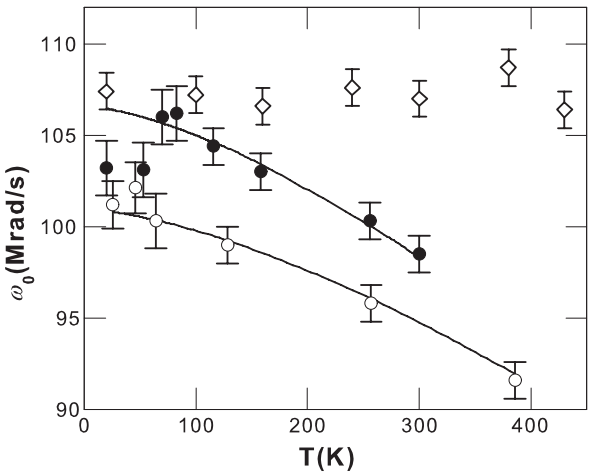

Figure 2. Temperature variation of quadrupole interaction frequency ω_0 for ^{111}Cd in CeScGe (○), PrScGe (●) and GdScGe (◇). The solid lines are fits to equation (6) reflecting a $T^{3/2}$ dependence.

The PAC spectra measured close to the ordering temperature of the samples show strong damping, indicating the onset of magnetic correlations. Examining the spectra for PrScGe it becomes evident that a static magnetic hyperfine field appears only below 80 K, i.e. the ferromagnetic ordering of Pr magnetic moments. We shall later discuss the magnetic behavior of PrScGe in the intermediate temperature range, i.e. between the antiferromagnetic transition at T_N = 140 K and the ferromagnetic ordering at T_c = 80 K. At low temperatures the ^{111}Cd nuclei experience the combined influence of magnetic and quadrupole interaction. As such the spectra recorded at 20 K were fitted for randomly oriented combined interaction. In the fitting procedure adopted here, the observed PAC spectra were fitted to $G_{22}(t)$ numerically simulated for different values of y and β. The procedure was iteratively repeated by changing the value of y and β in small steps over a range until the best fit determined from the condition of minimum χ^2 was obtained. The extracted hyperfine field parameters are listed in table 1. Figure 3 displays the temperature variation of the magnetic hyperfine field B_{hf} for ^{111}Cd in CeScGe, PrScGe and GdScGe. The spectra measured at 20 K yielded B_{hf} to be 18 kG, 43 kG and 188 kG for CeScGe, PrScGe and GdScGe, respectively. The magnitude of B_{hf} smoothly decreased with increasing temperature, vanishing above the magnetic ordering temperatures. The data extrapolated to B_{hf} = 0 yielded the ordering temperatures $T_c(T_N)$ = 40 K, 80 K and 340 K for the Ce, Pr and Gd alloys, respectively. While the ordering temperatures for Ce and Gd alloys are in agreement with bulk magnetization data, in PrScGe the magnetic hyperfine field does not set in at T_N = 140 K but starts to appear only below the ferromagnetic ordering temperature 80 K. Extrapolating the $B_{hf}(T)$ data to T = 0, the saturated hyperfine field $B_{hf}(0)$ of Cd in RScGe alloys was determined to be 21(2) kG, 45(2) kG and 189(1) kG for R = Ce, Pr and Gd alloys, respectively. The angle β between the magnetic and EFG axes was found to be close to 40° for all three cases studied. Assuming the EFG axis to be along the c direction of the unit cell, the observed values of β indicate that the rare-earth moments are non-collinear with respect to the crystallographic axes. Recently, Manfrinetti *et al* have determined the magnetic structure of PrScGe using the neutron diffraction method [21]. The measurements performed in single-crystal samples were

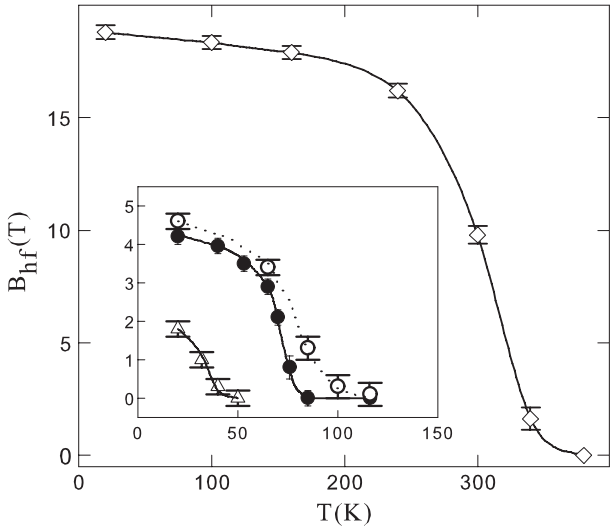

Figure 3. Magnetic hyperfine field B_{hf} as a function of temperature measured for ^{111}Cd in GdScGe (◊). Inset shows the data for CeScGe (△) and PrScGe (●). Open circles are data for PrScGe taken in external field of 5 kG. The lines through the data points are guides for the eyes.

Table 1. Summary of hyperfine parameters for ^{111}Cd in RScGe alloys; R = Ce, Pr and Gd. ω_0: quadrupole interaction frequency; magnetic hyperfine field B_{hf}; β: relative angle between the magnetic field and EFG.

Alloy	Temperature (K)	ω_0 (Mrad s^{-1})	B_{hf} (kG)	β (degree)
CeScGe	20	101.2(13)	18.0(20)	41(5)
	36	102.1(14)	10.0(20)	38(5)
	50	100.3(15)	0.3(10)	40(5)
	100	99.0(10)	0	
	200	95.8(10)	0	
	300	91.6(10)	0	
PrScGe	20	103.2(15)	42.0(15)	45(3)
	53	103.1(15)	35.0(18)	40(4)
	70	106.0(20)	21.0(20)	37(4)
	83	106.2(15)	0.6(20)	42(5)
	116	104.4(17)	0	
	158	103.0(12)	0	
	256	100.3(10)	0	
	300	98.5(10)	0	
GdScGe	20	107.4(10)	188.0(10)	42(3)
	100	107.2(10)	184.1(10)	39(4)
	160	106.6(13)	178.9(13)	45(3)
	240	107.6(16)	162.0(10)	40(3)
	300	107.0(12)	98.0(15)	38(4)
	380	108.7(10)	16.3(20)	43(4)
	430	106.4(10)	0	

reported to order in a ferrimagnetic structure below 60 K with Pr moments making an angle of 62° with respect to the crystallographic *c* axis [21]. Though the angle β derived from our PAC data differs from the value reported from neutron measurements, the results presented here qualitatively support the canted magnetic structure reported by Manfrinetti *et al* [21].

As mentioned above, bulk magnetization studies in PrScGe show the onset of an antiferromagnetic ordering at T_N = 140 K followed by a ferromagnetic transition at

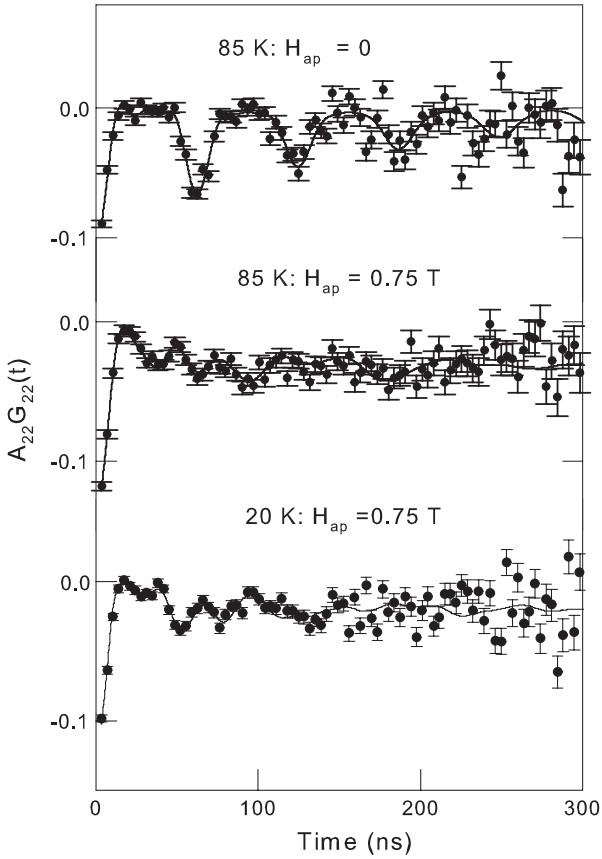

Figure 4. ^{111}Cd TDPAC spectra in PrScGe measured in zero applied field and in external field of 5 kG at 85 K.

T_c = 80 K. The hyperfine field of ^{111}Cd obtained from TDPAC measurements in zero applied field was observed to vanish near 80 K, indicating the loss of long range magnetic order. In order to examine the magnetic state of PrScGe on a local scale, measurements were carried out in an external magnetic field of 5 kG. The PAC spectra recorded at 85 K with and without an external field are shown in figure 4. It can be easily noticed that the spectrum in an applied field is qualitatively different from that in zero field, yielding a large B_{hf} = 1.3 T. The temperature dependence of B_{hf} in an applied field is shown in figure 3 (open circles). The observed large field-induced hyperfine field for $T > 80$ K indicates the presence of strong magnetic correlation above T_c. These results suggest that the Pr moments between T_c and T_N can be easily aligned by external fields like ferromagnets. This field-induced magnetic behavior of PrScGe would be consistent with ferrimagnetism reported from neutron diffraction measurements [21]. It should be pointed out that the hyperfine field of Cd between T_N = 140 K and T_{c1} = 85 K (AFM phase) remains zero even in the presence of an external field. Manfrinetti *et al* have shown that in the temperature range 85–140 K PrScGe orders antiferromagnetically with a magnetic moment of 1.72 μ_B on each Pr atom [21]. Since the hyperfine field at a non-magnetic probe nucleus arises from spin polarization of s-electrons by the neighboring magnetic atoms, for the tetragonal structure of PrScGe, with Pr atoms carrying equal but opposite moment, the B_{hf} for a Cd probe replacing the Sc site is expected to

vanish from symmetry considerations, which is reflected in our TDPAC measurements. However, for a ferrimagnetic spin arrangement with unequal Pr moments the spin density at the Cd probe does not vanish, giving rise to the small B_{hf} values seen in our PAC experiment.

At this point it is worthwhile to compare the magnetic hyperfine of Cd in RScGe with those observed in the corresponding pure metal. The magnetic hyperfine fields of ^{111}Cd in rare-earth metals and several intermetallic alloys have been measured by the TDPAC method [20, 22, 23]. In most of the cases studied, it has been found that the B_{hf} is proportional to the spin projection factor $(g_J - 1)J$, i.e. $B_{hf} = \text{const} \times (g_J - 1)J$, where g_J is the Landé g factor. Furthermore, considering that the RKKY interaction is the main mechanism for the magnetic interaction in rare-earth metals and compounds, the transferred hyperfine field at ^{111}Cd is expected to scale with the ratio $N\mu_{RE}/r^3$, where N is the number of near rare-earth atoms surrounding the Cd probe and r is the inter-atomic distance. Extrapolating the trend observed for Nd–Tm, the hyperfine field of ^{111}Cd in Pr metal is expected to be ≈3 T. For Ce metal the hyperfine field of Cd is expected to be even smaller—⩽1 T [22]. For Cd in Gd metal B_{hf} has been measured to be 340 kG. Using these values for elemental rare-earths and the inter-atomic distances obtained from x-ray diffraction measurements the B_{hf} of ^{111}Cd in CeScGe, PrScGe and GdScGe are expected to be ⩽1 T, ≈3 T and ≈10 T, respectively. In contrast, the measured B_{hf} values, particularly for PrScGe and GdScGe, turn out to be significantly higher. Similar enhancement in the hyperfine field of the Cd probe nucleus has been reported earlier for the ferromagnetic compound NdScGe [12]. It was suggested that spin polarization of conduction electrons, especially from the Sc d band polarized by the RE moment, might contribute to the magnetic interaction and the hyperfine field at Cd. We therefore feel that spin polarization of Sc d band electrons also play an important role in the magnetism of RScGe compounds, including CeScGe. The suggested Sc d band spin polarization is consistent with the results obtained from *ab initio* calculations discussed below.

Complimenting the experimental studies we have performed a series of *ab initio* calculations in pure and Cd-doped RScGe (R = Ce, Pr, Nd and Gd). The calculations were performed within density functional theory (DFT) [24–26], using the augmented plane waves + local orbitals (APW + lo) method [27, 28] as implemented in the WIEN2k package [29]. In the APW + lo method, the wavefunctions are expanded in spherical harmonics inside non-overlapping atomic spheres of radius R_{MT}, and in plane waves in the remaining space of the unit cell (=the interstitial region). The R_{MT} value was chosen to be 2.5 au for the rare-earth atoms including Sc. For the Ge atoms the R_{MT} value was taken to be 2.2 au. The maximum ℓ for the expansion of the wavefunction in spherical harmonics inside the spheres was taken to be $\ell_{max} = 10$. The plane wave expansion of the wavefunction in the interstitial region was made up to $K_{max} = 8.0/R_{MT}^{min} = 3.6$ au^{-1}. The charge density was Fourier-expanded up to $G_{max} = 16\sqrt{\text{Ryd}}$. In order to calculate the electric field gradient and magnetic hyperfine field of the Cd impurity in CeScGe and PrScGe, a $2 \times 2 \times 2$ supercell consisting of 8 units of RScGe was constructed with one of the Sc atoms substituted by Cd. For the sampling of the Brillouin zone, a special k-mesh equivalent to a $10 \times 10 \times 10$ mesh in the pure RScGe structure was used throughout. As the exchange–correlation functional, we have used the Perdew–Burke–Ernzerhof generalized gradient approximation (GGA) [30]. Calculations were also performed using the GGA+U method [31] with effective U, $U_{eff} = U - J$ values 0.40 Ryd, 0.43 Ryd, 0.49 Ryd and 0.53 Ryd for Ce, Pr, Nd and Gd, respectively, estimated using the empirical formula given in the literature [32]. The U_{eff} chosen for our cases are also in accordance with the values used in earlier calculations [33–37]. For both the cases (GGA and GGA + U) spin–orbit interaction was considered for the rare-earth atoms. All the calculations were performed using equilibrium lattice parameters obtained by minimizing the total energy as a function of cell volume, c/a ratio and internal coordinates of the rare-earth and Ge atoms, Z_R and Z_{Ge}, respectively. Lattice relaxation was considered at each stage to minimize the force on each atom to ⩽1 mRyd. For the pure materials, calculations were carried out for unpolarized (non-magnetic—NM) and spin polarized (magnetic) cases. For the magnetic cases, both parallel and antiparallel alignment of the RE spins, labeled as FM and AFM, respectively, were considered. Self-consistency of the calculations were determined with charge and energy convergence criteria 0.0001 and 0.01 mRyd, respectively.

Table 2. Summary of calculated structural properties of RScGe (R = Ce, Pr, Nd and Gd) alloys.

	CeScGe	PrScGe	NdScGe	GdScGe
a (Å)	4.3247	4.3053	4.2921	4.2453
a_{exp} (Å)	4.345	4.2976[a]	4.2901[a]	4.258
c/a	3.6843	3.6827	3.6835	3.6503
c/a_{exp}	3.6742	3.6867	3.6915	3.6476
Z_R	0.3220	0.3235	0.3234	0.3219
Z_R (exp)	0.3238	0.3225	0.3226	0.3228
Z_{Ge}	0.1219	0.1227	0.1237	0.1277
Z_{Ge} (exp)	0.1211	0.1212	0.1231	0.1265
Vol (Å)^3	298.013	293.884	291.253	279.286
B (GPa)	70.08	64.71	73.44	98.67

[a] Data taken from [21].

Figure 5 displays the total energy E_{tot} as a function of unit cell volume calculated for the RScGe (R = Ce, Pr, Nd and Gd) compounds. The structural properties obtained from minimization of E_{tot} as a function of volume, c/a ratio and internal coordinates of the rare-earth and Ge atoms are listed in table 2. The bulk modulus of the alloys was estimated by fitting the total energy as a function of volume to the Birch–Murnaghan equation of state [38] implemented in the WIEN2k program [29]. It is satisfying to note that the calculated lattice parameters closely agree with the experimental values. Following Moruzzi *et al* [39] the larger value of the bulk modulus indicates higher θ_D for GdScGe in comparison to the other alloys studied. The larger θ_D, implying smaller mean square displacement ($\langle r^2 \rangle$), could qualitatively explain the weak temperature dependence of the quadrupole interaction frequency in GdScGe.

Table 3. Summary of calculated results for RScGe (R = Ce, Pr, Nd and Gd). $\mu_{tot}(\mu_B)$: total moment per formula unit; $\mu_R(\mu_B)$: sum total of the spin and orbital moments of the rare-earth atoms including spin polarization of the 5d shell shown as μ_{5d}; $\mu_{Sc}(\mu_B)$: moment on Sc; $\mu_{Ge}(\mu_B)$: moment on Ge atoms; magnetic energy E_M(Ryd) = E(FM/AFM) − E(NM).

	GGA					GGA + U				
Alloy	μ_{tot}	μ_R	μ_{Sc}	μ_{Ge}	E_M (Ryd)	μ_{tot}	μ_R	μ_{Sc}	μ_{Ge}	E_M (Ryd)
CeScGe(NM)	0				0					0
CeScGe(FM)	1.06	0.98	0.13	−0.05	−0.003 11	0.99	0.92 μ_{orb} = 1.75 μ_{spin} = −0.90 μ_{5d} = 0.07	0.10	−0.03	−0.00387
CeScGe(AFM)	0.13	0.75; −0.66	0.08	−0.04	−0.006 77	0.12	0.86; −0.91 μ_{orb} = 1.56; −1.54 μ_{spin} = −0.75; 0.69 μ_{5d} = 0.06; −0.06	0.08	−0.03	−0.00739
PrScGe(NM)	0				0					0
PrScGe(FM)	2.43	2.21	0.16	−0.06	−0.085 11	3.09	2.98 μ_{orb} = 4.79 μ_{spin} = −1.96 μ_{5d} = 0.13	0.16	−0.05	−0.08427
PrScGe(AFM)	0.41	2.19; −1.98	0.14	−0.04	−0.103 64	0.58	2.54; −2.08 μ_{orb} = 4.35; −3.89 μ_{spin} = −1.94; 1.93 μ_{5d} = 0.13; −0.12	0.15	−0.03	−0.09294
NdScGe(NM)	0				0					0
NdScGe(FM)	3.41	3.27	0.19	−0.05	−0.333 47	3.22	3.03 μ_{orb} = 5.87 μ_{spin} = −3.02 μ_{5d} = 0.18	0.23	−0.04	−0.35236
NdScGe(AFM)	0.38	3.36; −3.17	0.19	−0.05	−0.128 36	0.18	2.92; −2.95 μ_{orb} = 5.68; 5.73 μ_{spin} = −2.93; −2.95 μ_{5d} = 0.17; −0.17	0.20	−0.05	−0.09172
GdScGe(NM)	0				0					0
GdScGe(FM)	7.42	7.19	0.29	−0.06	−0.850 71	7.74	7.44 μ_{orb} = 0.0 μ_{spin} = 7.02 μ_{5d} = 0.42	0.34	−0.04	−1.04663

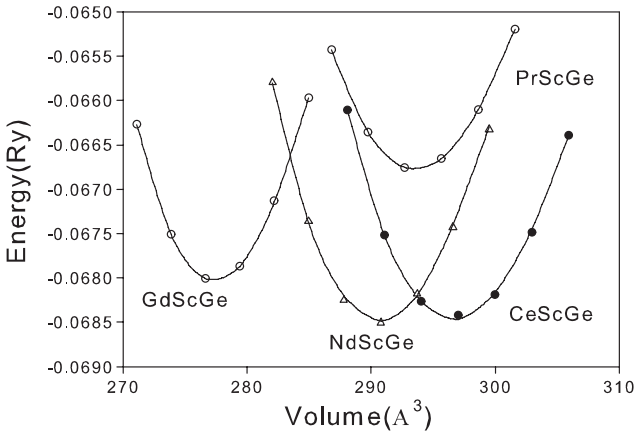

Figure 5. Variation of total energy as a function of unit cell volume calculated for RScGe compounds for R = Ce, Pr, Nd and Gd. For convenience of display, the vertical axis for each case has been shifted by an arbitrary value.

Next we come to the magnetic properties of pure RScGe compounds and examine their ground state by comparing the total energies E_{tot} obtained from unpolarized and spin polarized (FM and AFM) calculations. The results are listed in table 3. From the results shown in table 3 it can be seen that, in the case of CeScGe and PrScGe, the solutions with antiparallel RE moments (AFM) have lower total energy compared to the ferromagnetic or the non-magnetic cases. Furthermore, one can notice that the Ce/Pr atoms have unequal magnetic moments, which indicates that the ground state for these alloys are ferrimagnetic. In contrast, the calculated E_{tot} reveal ferromagnetic ground states for NdScGe and GdScGe. The magnetic ground states predicted from our DFT calculations agree with the magnetic structures proposed from recent neutron diffraction measurements [21, 43]. It is worthwhile noting that, in the case of CeScGe, we find that the total energy of the non-magnetic and magnetic solutions are close to each other with an energy difference of ± ≈4 mRyd, indicating competing magnetic interactions, in agreement with the results reported by Shigeoka *et al* [40]. The results obtained for PrScGe also suggest competition between ferro- and antiferromagnetic states. Considering the fact that GdScGe having a large ferromagnetic ordering temperature has a smaller unit cell, it is important to check if the ground state of the alloys, especially CeScGe and PrScGe, depends on the unit cell volume. For this, additional calculations were performed

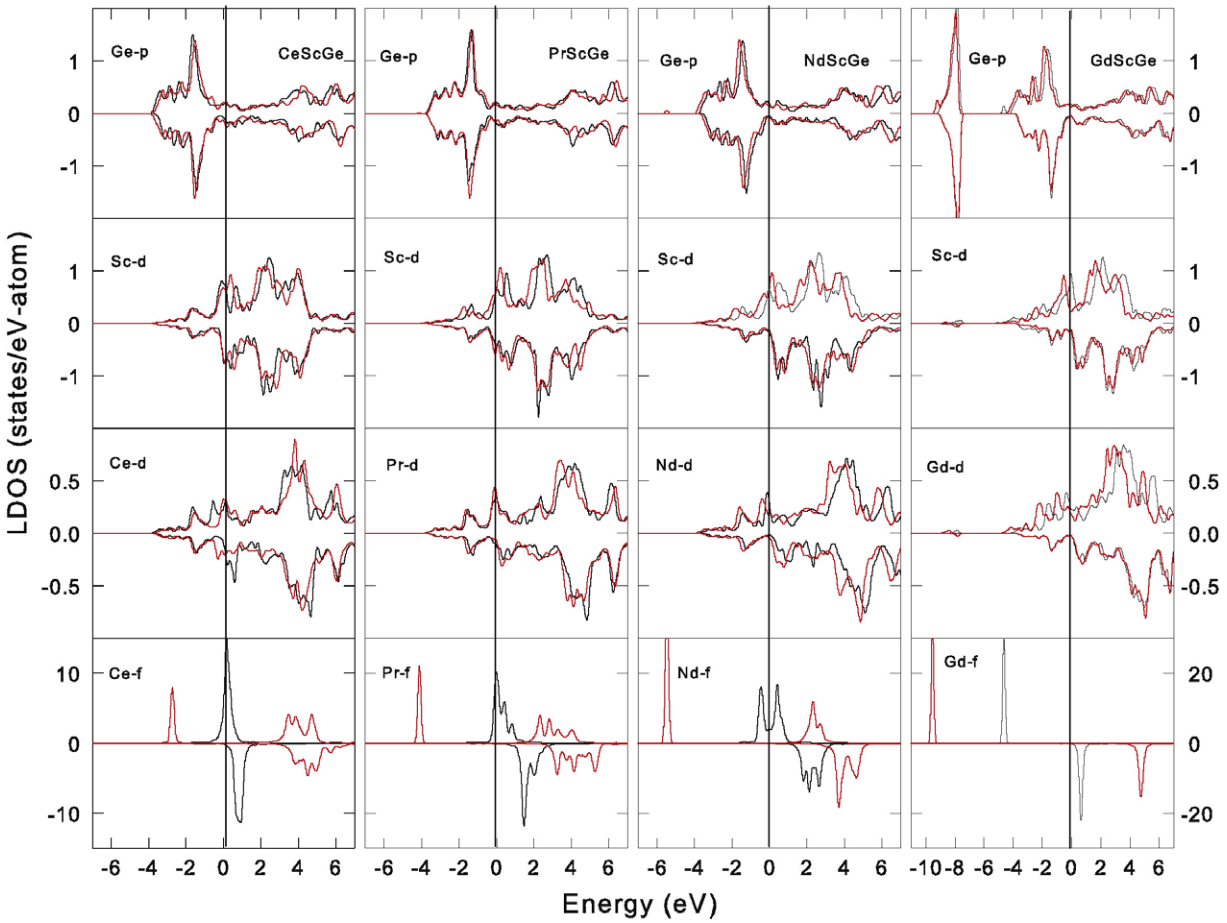

Figure 6. Atom-and spin-projected local density of states for RScGe compounds; R = Ce, Pr, Nd and Gd. The vertical dotted line represents the position of the Fermi energy E_F. The solid black lines represent the LDOS obtained from GGA ($U = 0$) calculations while the red lines correspond to the results of the GGA + U method (see text).

(This figure is in colour only in the electronic version)

for CeScGe and PrScGe with reduced unit cell parameters, chosen to match the values for GdScGe. The total energies of the AFM cases, relative to the non-magnetic calculations, were still found to be lower compared to the respective FM cases by ≈5 mRyd in CeScGe and ≈10 mRyd for PrScGe. It should also be mentioned that, for both cases, we did not find much difference in the 4f moments, although the 5d and Sc d moments, especially for CeScGe, showed a noticeable reduction. We are thus confident that the unit cell volume does not have a serious influence on the calculated results discussed below.

Figure 6 displays the atom-and spin-projected local density of states (LDOS) for the RScGe (R = Ce, Pr, Nd and Gd) compounds obtained from GGA as well as GGA + U calculations. Without the orbital polarization ($U = 0$) the 4f states of the rare-earth atoms in CeScGe, PrScGe and NdScGe are located near the Fermi energy showing an exchange splitting of 0.65 eV, 1.45 eV and 2.1 eV, respectively. In the case of GdScGe, the majority and minority 4f DOS, far removed from E_F, exhibit an exchange splitting of 7 eV. The LDOS obtained from GGA + U calculations show narrow 4f bands with the majority states located at −2.4 eV, −3.8 eV, −5.0 eV and −9.0 eV in CeScGe, PrScGe, NdScGe and GdScGe, respectively. The calculated magnetic moments are listed in table 1. It can be noticed that the 4f moments, except CeScGe, are close to the saturation moment $\mu_s = g_J J$ of Hund's rule ground state of the respective trivalent rare-earth ions. In the case of CeScGe the 4f moment came out to be close to 1 μ_B, which is significantly smaller than the saturation value 2.15 μ_B of $J = 5/2$ Ce^{3+} ions. Recently, Shigeoka *et al* calculated the band structure of CeScGe within the local spin density approximation (LSD) using the LMTO method [40]. The Ce moments for the ferro- and antiferromagnetic states were found to be 0.62 μ_B and 0.37 μ_B, respectively. The moment values obtained from our GGA and GGA + U calculations, though higher compared to those reported by Shigeoka *et al* [40], agree with the experimental value reported from high field magnetization data [3, 21, 43]. Apart from the spin and orbital moments of the RE atoms, an analysis of partial occupation number for different orbitals of the rare-earth atoms yielded sizable magnetic moments from the 5d band whose magnitude was found to increase from ≈0.06 μ_B for CeScGe to 0.42 μ_B in GdScGe. This RE 5d moments, arising mainly due to intra-atomic f–d exchange interaction, are found to be parallel to the rare-earth moments, consistent with the models proposed by Campbell

and Brooks [41, 42]. Based on heuristic arguments [41] and first-principles calculations [42] it has been shown that the 5d moment in the first half of the rare-earth series is parallel to the 4f moment, while an antiparallel alignment was found in the latter half. For the ground states determined by the total energy the net magnetic moment of the rare-earth atoms is estimated to be $\approx 1\mu_B$ for CeScGe, 2.5 μ_B for PrScGe, 3.03 μ_B NdScGe and 7.44 μ_B for GdScGe (see table 1). We would like to note that for the AFM cases, particularly for PrScGe, the magnetic moments of the two inequivalent RE atoms came out to be 2.54 μ_B and 2.08 μ_B, suggesting a ferrimagnetic ground state. This is in agreement with the magnetic structure suggested from low temperature neutron diffraction measurements [21] although the moment values are somewhat different. It is satisfying to note that the RE moments obtained from our *ab initio* calculations closely agree with the experimental values reported in the literature [3, 6, 21, 43].

In addition to the spin and orbital moments of the rare-earth atoms, we find a sizable magnetic moment at the Sc site of the RScGe alloys. The moment on Sc, arising mainly from spin polarization of Sc 3d band electrons, increases from $\approx$0.07 μ_B in CeScGe to 0.34 μ_B for GdScGe. The spin polarization of the Sc 3d band in RScGe compounds observed from our DFT calculations support the earlier conclusion inferred from the hyperfine field results obtained from TDPAC measurements. From the results presented in table 3 it can be seen that the calculated μ_{Sc} roughly scale with the magnetic moments of the rare-earth atoms. Furthermore, in all the cases studied the Sc moments are ferromagnetically coupled to the RE 4f moment, in accordance with the model predictions by Campbell and Brooks [41, 42]. Considering that the unpolarized calculations show a small density of state at the Sc site ($N(E_F)$(Sc) $\leqslant$ 1 states/eV atom) the Stoner condition [44] for the formation of a local moment on Sc would not be satisfied. The observed moment on the Sc atoms is therefore likely to be induced by the RE 4f moments. It should be noted that the 4f moment of the rare-earth also induces strong spin polarization of its own 5d band electrons which are reflected by the sizable magnitude of μ_{5d} shown in table 3. This polarized RE 5d band electrons strongly hybridized with the Sc 3d band can lead to large induced moment at the Sc atoms. It is worthwhile mentioning that electronic structure calculations performed for GdTiGe and GdTiSi have also revealed large induced moments on Ti atoms, indicating strong spin polarization of the Ti 3d band in these alloys [7]. We believe spin polarization of Sc 3d band electrons plays an important role towards the occurrence of high ordering temperatures in RScGe alloys. To illustrate this we start under the premise that magnetic ordering in rare-earth metals and alloys arise due to the RKKY interaction. According to this model, the interatomic exchange interaction between 4f moments is governed mainly by the range and strength of conduction electron spin polarization which varies as $\cos(2k_F r)/r^3$, with r being the interatomic distance between 4f atoms and k_F the Fermi wavevector. The 5d wavefunction having the largest overlap with the 4f state contributes the most to the conduction electron spin polarization (see table 3). The extended 5d wavefunction overlapping with the neighboring RE atoms also enables the interatomic f–f interaction. It should be noted that the k_f for the RScGe compounds, estimated from the calculated Fermi energies ($k_f = E_F/\hbar$), are close to the values obtained for the respective rare-earth metals. Therefore, discounting the role of Sc d band electrons, the f–f interaction is expected to decrease with increasing distance. Thus, because of the larger RE–RE separation the f–f coupling in RScGe compounds is expected to be weaker compared to the corresponding rare-earth elements, resulting in lower transition temperatures. In contrast, the transition temperatures in RScGe compounds have been observed to be higher than the rare-earth metals. The spin polarized broad 3d band of Sc strongly overlapping with RE 5d electrons, however, can successfully bridge this gap and increase the exchange interaction between 4f moments. We therefore suggest that spin polarization of Sc 3d band electrons, via spin polarized 5d electrons of rare-earths, enables long range RKKY interaction, giving rise to high magnetic ordering temperatures as observed in RScGe compounds. It should be mentioned that a similar mechanism has been proposed recently by Haskel *et al* to explain the high magnetic ordering temperatures in $Gd_5(Ge_{1-x}Si_x)_4$ alloys [45].

Next we come to the hyperfine fields of the Cd impurity substituted at the Sc site in RScGe (R = Ce, Pr, Nd) alloys. Calculations were performed for non-magnetic (without spin polarization) as well as magnetic (with spin polarization) cases. For the magnetic cases we restricted to the lowest energy magnetic states—ferro- or antiferromagnetic—obtained for the pure material discussed above. In the case of CeScGe, because of the near-degeneracy of magnetic states (see the discussion above), calculations were made for both ferro- and antiferromagnetic states. The results are summarized in table 4. For the non-magnetic cases, only the electric hyperfine interaction is possible and the calculated electric field gradient can be compared with the experimental results obtained for temperatures $T > T_C(T_N)$. From the non-magnetic calculations the principal component of the EFG tensor V_{zz} at the Cd impurity substituted at the Sc site in the RScGe structure was found to be 4×10^{21} V m^{-2}, 4.2×10^{21} V m^{-2}, 4.5×10^{21} V m^{-2} and 4.6×10^{21} V m^{-2} in Ce, Pr, Nd and Gd compounds. These V_{zz} values closely agree with our TDPAC results obtained for $T > T_c$. The results support the assumption that the ^{111}Cd probe in our TDPAC experiments occupies the Sc site in RScGe compounds. The spin polarized calculations, yielded $V_{zz} = 5.3 \times 10^{21}$ V m^{-2} for CeScGe, agreeing with the experimental data at 20 K. For PrScGe, NdScGe and GdScGe, however, the magnetic calculations yielded slightly smaller EFG values, qualitatively in agreement with the features observed from the experimental measurements (see figure 2). Secondly, the magnetic calculations yielded a small but finite asymmetry η of the EFG tensor consistent with the breaking of local symmetry due to ordering of the RE moments. This small change in local symmetry, however, could not be detected without ambiguity from our low temperature PAC spectra showing complex combined interaction patterns. Coming to the magnetic interaction, the magnetic hyperfine fields of the Cd impurity in RScGe compounds were calculated using the

Table 4. Summary of calculated results for Cd-doped RScGe (R = Ce, Pr, Nd) obtained from GGA and GGA + U calculations. $\mu_{RE}(\mu_B)$: spin magnetic moment of rare-earth atoms; $\mu_{Sc}(\mu_B)$: magnetic moment on Sc; $\mu_{Ge}(\mu_B)$: moment on Ge atoms; $V_{zz}^{Cd} \times 10^{21}$ V m^{-2}: principal component of electric field gradient at Cd site; η: asymmetry of EFG at Cd site; B_{hf}^{Cd}(cal)(kG): magnetic hyperfine field of Cd impurity. For comparison, the experimental values of the saturation hyperfine field of Cd $B_{hf}^{Cd}(0)$(kG) are shown in the last column.

Alloy	μ_{RE}	μ_{Sc}	μ_{Ge}	V_{zz}^{Cd}	η	B_{hf}^{Cd} (cal)	B_{hf}^{Cd} (expt)
CeScGe(NM)				−4.04	0.0		
CeScGe(FM)(GGA)	0.94	0.08	−0.03	−5.48	0.04	−4.2	
(GGA + U)	0.95	0.10	−0.03	−5.26	0.01	−4.9	21 ± 2
CeScGe(AFM)(GGA)	0.67	0.08	−0.03	−5.18	0.06	15.5	
(GGA + U)	0.81	0.08	−0.04	−5.34	0.06	20.0	
PrScGe(NM)				−4.23	0.00		
PrScGe(AFM)(GGA)	2.11	0.14	−0.04	−3.77	0.10	35.7	
(GGA + U)	2.35	0.15	−0.04	−3.62	0.07	40.4	45 ± 2
NdScGe(NM)				−4.41	0.00		
NdScGe(FM)(GGA)	3.48	0.21	−0.05	−3.49	0.12	−56.8	
(GGA + U)	3.49	0.23	−0.06	−3.45	0.11	−64.2	85 ± 1
GdScGe(NM)				−4.37	0.00		
GdScGe(FM)(GGA)	7.17	0.27	−0.06	−4.52	0.08	−144.6	
(GGA + U)	7.46	0.32	−0.06	−4.49	0.05	−167.6	189 ± 1

scalar relativistic formula of Blugel *et al* [46] implemented within the WIEN2k program [29]. It can be noticed (see table 4) that the B_{hf} values calculated within GGA as well as GGA + U methods closely agree with the experimental results obtained from TDPAC measurements.

In summary, we have made microscopic investigations of the magnetic interactions in rare-earth intermetallic compounds RScGe (R = Ce, Pr and Gd) by measuring hyperfine fields of ^{111}Cd using the TDPAC technique. Supplementing the experimental studies we have also made *ab initio* calculations within density functional theory (DFT). The Cd nuclei occupying the Sc site show high magnetic hyperfine fields with saturation values $B_{hf}(0)$ = 2.1 T, 4.5 T and 18.9 T in CeScGe, PrScGe and GdScGe, respectively. By comparing the results with the hyperfine field data of Cd in rare-earth metals and estimations from the RKKY model, we find evidence for the presence of additional spin density at the probe nucleus, possibly due to spin polarization of Sc d band electrons. *Ab initio* calculations for pure and Cd-doped RScGe compounds with R = Ce, Pr, Nd and Gd using the full potential linearized augmented plane wave (FLAPW) method show ferrimagnetic ground states for CeScGe and PrScGe while NdScGe and GdScGe are predicted to be ferromagnetic. The calculated magnetic ground states are in agreement with neutron diffraction results. In addition, we find a sizable magnetic moment at the Sc site, increasing from ≈0.08 μ_B in CeScGe to 0.34 μ_B in GdScGe, confirming the spin polarization of Sc d band electrons. We believe spin polarization of Sc 3d band electrons, overlapping with the spin polarized 5d band of the rare-earths, enables a long range RKKY interaction between 4f moments in RScGe compounds, leading to high magnetic ordering temperatures. Further experimental studies using the XMCD technique will be helpful to get a direct measure of Sc 3d spin polarization in RScGe alloys.

Acknowledgments

We thank Professor S K Dhar for providing the samples used in this work. We also thank S M Davane for assistance during TDPAC measurements.

References

[1] Szytula A 1991 *Handbook of Magnetic Materials* vol 6, ed K H J Buschow (Amsterdam: North-Holland) chapter 2 p 86
[2] Manfrinetti P, Pani M, Palenzona A, Dhar S K and Singh S 2002 *J. Alloys Compounds* **334** 9
[3] Canfield P C, Thompson J D and Fisk Z 1991 *J. Appl. Phys.* **70** 5992
[4] Singh S, Dhar S K, Mitra C, Paulose P, Manfrinetti P and Palenzona A 2001 *J. Phys.: Condens. Matter* **13** 3753
[5] Singh S, Dhar S K, Manfrinetti P, Palenzona A and Mazzone D 2004 *J. Magn. Magn. Mater.* **269** 113
[6] Nikitin S A, Ovtchenkova I A, Skourski Yu V and Morozkin A V 2002 *J. Alloys Compounds* **345** 50
[7] Skorek G, Deniszczyk J, Szade J and Tyszka B 2001 *J. Phys.: Condens. Matter* **13** 6397
[8] Schatz G and Weidinger A 1996 *Nuclear Condensed Matter Physics–Nuclear Methods and Applications* (New York: Wiley)
[9] Mahnke H E 1989 *Hyperfine Interact.* **49** 77
[10] Karlsson E B 1995 *Solid State Phenomena as Seen by Muons, Protons and Excited Nuclei* (Oxford: Clarendon)
[11] Colley M G, Chaplin D H, Swan D E and Wilson G V H 1975 *J. Phys. F: Met. Phys.* **5** L80
Colley M G, Chaplin D H, Swan D E and Wilson G V H 1976 *J. Phys. F: Met. Phys.* **6** 131
[12] Mishra S N and Dhar S K 2004 *J. Phys.: Condens. Matter* **16** 635
[13] Raghavan P 1989 *At. Data Nucl. Data Tables* **42** 189
[14] Frauenfelder H and Steffen R M 1965 *Alpha, Beta- and Gamma-Ray Spectroscopy* ed K Siegbahn (Amsterdam: North-Holland)
[15] Dogra R, Junquiera A C, Saxena R N, Carbonari A W, Mestnik-Filho J and Moralles M 2001 *Phys. Rev.* B **63** 224104
[16] Krishnamurthy V V, Habenicht S, Lieb K-P, Uhrmacher M and Winzer K 1997 *Phys. Rev.* B **56** 355
[17] Alder K and Steffen R M 1963 *Phys. Rev.* **129** 1199
[18] Kaufmann E N and Vianden R J 1979 *Rev. Mod. Phys.* **51** 161
[19] Torumba D, Parlinski K, Rots M and Cottenier S 2006 *Phys. Rev.* B **74** 144304
[20] Forker M and de la Presa P 2007 *Phys. Rev.* B **76** 115111
[21] Manfrinetti P, Morozkin A V, Isnard O, Henry P and Palenzona A 2008 *J. Alloys Compounds* **450** 86
[22] Forker M, Freise L and Simon D 1989 *Solid State Commun.* **71** 1169

[23] de la Presa P, Forker M, Cavalcante J Th and Ayala A P 2006 *J. Magn. Magn. Matter.* **306** 292
[24] Hohenberg P and Kohn W 1964 *Phys. Rev.* **136** 864
[25] Kohn W and Sham L J 1965 *Phys. Rev.* **140** A1133
[26] Cottenier S 2002 *Density Functional Theory and the Family of (L)APW-Methods: A Step-By-Step Introduction* Instituut voor Kern-en Stralingsfysica, K U Leuven, Belgium ISBN 90-807215-14
[27] Sjöstedt E, Nordström L and Singh D J 2000 *Solid State Commun.* **114** 15
[28] Madsen G K H, Blaha P, Schwarz K, Sjöstedt E and Nordström L 2001 *Phys. Rev.* B **64** 195134
[29] Blaha P, Schwarz K, Madsen G K H, Kvasnicka D and Luitz J 1999 *WIEN2k: An Augmented Plane Wave + Local Orbitals Program for Calculating Crystal Properties* (Karlheinz Schwartz, Technische Universität, Wien, Austria)
[30] Perdew J P, Burke K and Ernzerhof M 1996 *Phys. Rev. Lett.* **77** 3865
[31] Anisimov V I, Zaanen J and Andersen O K 1991 *Phys. Rev.* B **44** 943
Solovyev I V, Dederichs P H and Anisimov V I 1994 *Phys. Rev.* B **50** 16861
Solovyev I V, Liechtenstein A I and Terakura K 1998 *Phys. Rev. Lett.* **80** 5758
Petukhov A G, Mazin I I, Chioncel L and Lichtenstein A I 2003 *Phys. Rev.* B **67** 153106
[32] van der Marel D and Sawatzky G A 1988 *Phys. Rev.* B **37** 10674
[33] Svane A, Trygg J, Johansson B and Eriksson O 1997 *Phys. Rev.* B **56** 7143
[34] Petersen M, Hafner J and Marsman M 2006 *J. Phys.: Condens. Matter* **18** 7021
[35] Torumba D, Novak P and Cottenier S 2008 *Phys. Rev.* B **77** 155101
[36] Loschen C, Carrasco J, Neyman K M and Illas F 2007 *Phys. Rev.* B **75** 035115
[37] Seo D-K 2007 *Phys. Rev.* B **76** 033102
[38] Birch F 1947 *Phys. Rev.* **71** 809
Murnaghan F D 1951 *Finite Deformation of an Elastic Solid* (New York: Wiley)
[39] Moruzzi V L, Janak J F and Schwarz K 1988 *Phys. Rev.* B **37** 790
[40] Shigeoka T, Yokoyama M, Kosaka M, Uwatoko Y, Furugen M, Ishida S and Asano S 2000 *Physica* B **281/282** 96
[41] Campbell I A 1972 *J. Phys. F: Met. Phys.* **2** L47
[42] Brooks M, Eriksson O and Johansson B 1989 *J. Phys.: Condens. Matter* **1** 5861
[43] Cadogan J, Ryan D H, Gagnon R and Voyer C J 2005 *J. Appl. Phys.* **97** 10A916
[44] Stoner E C 1938 *Proc. R. Soc.* A **165** 372
Beuerle T, Hummler K, Elaässer C and Fäahnle M 1994 *Phys. Rev.* B **49** 8802
[45] Haskel D, Lee Y B, Harmon B N, Islam Z, Lang J C, Srajer G, Mudryk Ya, Gschneidner K A Jr and Pecharsky V K 2007 *Phys. Rev. Lett.* **98** 247205
[46] Blügel S, Akai H, Zeller R and Dederichs P H 1987 *Phys. Rev.* B **35** 3271